eNeuro

Research Article: New Research | Sensory and Motor Systems

Modulation of rhythmic activity in mammalian spinal networks is dependent on excitability state

State-dependent modulation of spinal motor networks

Simon A. Sharples[1] and Patrick J. Whelan[1,2]

[1]*Hotchkiss Brain Institute, University of Calgary, Calgary, AB, Canada T2N 4N1*
[2]*Department of Comparative Biology and Experimental Medicine, University of Calgary, Calgary, AB, Canada, T2N 4N1*

DOI: 10.1523/ENEURO.0368-16.2017

Received: 12 December 2016

Revised: 11 January 2017

Accepted: 12 January 2017

Published: 19 January 2017

Funding: Gouvernement du Canada | Canadian Institutes of Health Research (CIHR)
501100000024

Funding: Gouvernement du Canada | Natural Sciences and Engineering Research Council of Canada (NSERC)
501100000038

Funding: Alberta Innovates - Health Solutions (AIHS)
501100000145

Funding: Gouvernement du Canada | Natural Sciences and Engineering Research Council of Canada (NSERC)
501100000038

Funding: Hotchkiss Brain Institute, University of Calgary (HBI, U of C)
100009003

Conflict of Interest: Authors report no conflict of interest.

Authors Contributions: S.A.S performed experiments and analyzed the data. S.A.S., and P.J.W. interpreted results of experiments, prepared figures, drafted, revised the manuscript and approved the final version of the manuscript. P.J.W. conceived and designed the research.

Funding for S.A.S was provided by the Natural Sciences and Engineering Research Council of Canada (NSERC-PGS-D), Alberta Innovates Health Solutions (AIHS), and a Dr. T. Chen Fong Doctoral Scholarship from the Hotchkiss Brain Institute. This research is supported by grants provided by the Canadian Institute of Health Research (P.J.W) and a NSERC Discovery grant (P.J.W).

Correspondence: Patrick Whelan, HMRB 168, 3310 Hospital Drive NW, Calgary, Alberta, T2N 4N1, CANADA. Email: whelan@ucalgary.ca

Cite as: eNeuro 2017; 10.1523/ENEURO.0368-16.2017

Title: Modulation of rhythmic activity in mammalian spinal networks is dependent on excitability state

Running Title: State-dependent modulation of spinal motor networks

Authors: Simon A. Sharples[1] and Patrick J. Whelan[1,2,*]

Affiliations: [1] Hotchkiss Brain Institute, University of Calgary, Calgary, AB, Canada, T2N 4N1 [2]Department of Comparative Biology and Experimental Medicine, University of Calgary, Calgary, AB, Canada, T2N 4N1

Number of pages: 31

Number of figures: 9

Number of words: Abstract (206), Introduction (611), Discussion (1561)

Correspondence:
Dr. Patrick Whelan
HMRB 168,
3310 Hospital Drive NW
Calgary, Alberta, T2N 4N1
CANADA
whelan@ucalgary.ca

Disclosures: No conflicts of interest, financial or otherwise, are declared by the authors(s).

Acknowledgements: We would like to acknowledge Jillian Ejdrygiewicz and Claude Viellet for their technical assistance during the completion of this work. We would also like to acknowledge Dr. Tuan Bui for helpful comments on the manuscript, Dr. Celine Jean-Xavier for helpful discussions, and Kyle Mayr for assisting with figure 8. Spinal Core software was a kind gift from Prof A. Lev-Tov (Hebrew University).

Contributions: S.A.S performed experiments and analyzed the data. S.A.S., and P.J.W. interpreted results of experiments, prepared figures, drafted, revised the manuscript and approved the final version of the manuscript. P.J.W. conceived and designed the research.

Grants: Funding for S.A.S was provided by the Natural Sciences and Engineering Research Council of Canada (NSERC-PGS-D), Alberta Innovates Health Solutions (AIHS), and a Dr. T. Chen Fong Doctoral Scholarship from the Hotchkiss Brain Institute. This research is supported by grants provided by the Canadian Institute of Health Research (P.J.W) and a NSERC Discovery grant (P.J.W).

Abstract:

Neuromodulators play an important role in activating rhythmically-active motor networks; however, what remains unclear are the network interactions whereby neuromodulators recruit spinal motor networks to produce rhythmic activity. Evidence from invertebrate systems has demonstrated that the effect of neuromodulators depends on the pre-existing state of the network. We explored how network excitation state affects the ability of dopamine to evoke rhythmic locomotor activity in the neonatal mouse isolated spinal cord. We found that dopamine can evoke unique patterns of motor activity that are dependent on the excitability state of motor networks. Different patterns of motor activity ranging from tonic, non-rhythmic activity to multi-rhythmic, non-locomotor activity to locomotor activity were produced by altering global motor network excitability through manipulations of the extracellular potassium and bath NMDA concentration. A similar effect was observed when network excitation was manipulated during an unstable multi-rhythm evoked by a low concentration (15 µM) of 5-HT – suggesting our results are not neuromodulator specific. Our data show in vertebrate systems that modulation is a two-way street and that modulatory actions are largely influenced by the network state. The level of network excitation can account for variability between preparations and is an additional factor to be considered when circuit elements are removed from the network.

Keywords: dopamine, spinal cord, rhythmicity, motor systems, locomotion, state-dependence

Significance Statement:

We show that as in the invertebrate systems the action of monoamine modulators on rhythmic motor networks of the mammalian spinal cord is state-dependent. Our work shows that neuromodulation in the spinal cord is fundamentally linked to the excitability state of the network. These findings have broad significance on mammalian network function since variations in network excitation can account for 1) diversity of neuromodulator function, 2) is an additional factor that must be considered when circuit elements are removed from a network to infer network function and 3) can account for variability often found between experimental preparations.

Introduction

Rhythmic motor behaviours mediate a number of functions essential to survival including breathing (Baghdadwala et al., 2016, Smith et al., 1991), feeding (Blitz and Nusbaum, 2012, Stadele et al., 2015) and locomotion (Gordon and Whelan, 2006, Grillner et al., 2008, Kiehn, 2016, Sillar et al., 2014). In vertebrates, neuronal networks within the spinal cord control rhythmic movements of the limbs and axial musculature to produce various forms of locomotion (Hultborn and Nielsen, 2007, Kiehn, 2016, Kimura et al., 2013, Roberts et al., 2012). While these networks have the capacity to function in isolation, normally they are modulated by inputs from the brain (Sharples et al., 2015, Koblinger et al., 2014, Miles and Sillar, 2011) brainstem (Bouvier et al., 2015, Hentall et al., 2003, Jordan et al., 2008, van den Pol, 1999), and by sensory feedback from the limbs (Whelan et al., 1995). Collectively these inputs endow these networks with the flexibility to produce diverse patterns of rhythmicity to suit the task at hand (Jordan et al., 2008, Marder et al., 2015, Sillar et al., 2014). Although evoked rhythms in the spinal cord have been characterized by others including our group, and diversity reported, we are not aware of this diversity being explained in terms of a modulatory-excitation state space (Barriere et al., 2005, Cowley and Schmidt, 1997, Gozal et al., 2014, Heckman and Johnson, 2014, Puhl and Mesce, 2008, Madriaga et al., 2004, Gordon and Whelan, 2006, Christie and Whelan, 2005, Humphreys and Whelan, 2012, Pearson et al., 2003).

The importance of excitation state is evident from examples provided in the small circuits of the stomatogastric nervous system whereby different motor patterns can be modelled as a function of balanced synaptic weights as well as intrinsic properties (Gutierrez et al., 2013, Gutierrez and Marder, 2014). The range of motor patterns generated as a function of varying circuit properties has been termed the circuit state or parameter space. Based on this, it has been proposed that modulation of circuit output is state-dependent and that the influence of a neuromodulator is linked to the relative position of the circuit within its parameter space. Several lines of evidence demonstrates that specific

86 motor patterns can also be achieved through multiple or degenerate mechanisms (Marder et al., 2014,
87 Gutierrez et al., 2013, Prinz et al., 2004).

88 We show that as in the invertebrate systems (Marder et al., 2014, Bargmann, 2012), the action of
89 monoamine modulators on rhythmic motor networks of the mammalian spinal cord is state-dependent.
90 We explore how network excitation state influences the modulatory effect of dopamine on
91 rhythmically-active motor networks in the isolated spinal cord of neonatal mice. This model is
92 advantageous since elements of the circuit have been genetically-defined, the motor output is well
93 characterized by several labs, and it is starting to be mathematically modelled. Broadly speaking, our
94 data suggest that it is important to consider modulation as a two-way street; modulatory actions are
95 largely influenced by the network state. Our results have functional implications in pathological
96 instances such as in Multiple Sclerosis, spinal cord injury, and stroke where spinal cord excitability and
97 stepping performance are compromised. Furthermore, the irregular rhythmic movements we report
98 here may be manifest in neonatal rodents while spinal networks are maturing and descending
99 projections developing. At this time, the neonate must still make movements to move towards the
100 mother. These movements tend to be erratic compared to full-fledged stepping that occurs around P9-
101 10 when complete weight-support is realized. Our data also function to provide a reference which
102 investigators can use to interpret variability in rhythmic patterns observed using isolated spinal cord
103 preparations. A portion of these results have been published in abstract form (Sharples and Whelan,
104 2015).

105 **Methods**

106 *Ethical approval & animals*

Experiments were performed on male and female neonatal C57/B6 mice of 0-4 days old (P0-P3; N=82). All procedures used were approved by the University of Calgary Health Sciences Animal Care Committee.

Tissue preparation:

Animals were anaesthetized by cooling, decapitated and eviscerated to expose the vertebral column. The remaining tissue was placed ventral side up in a dissection chamber filled with room-temperature carbogenated (95% O_2, 5% CO_2) artificial cerebrospinal fluid (aCSF) in mM (128 NaCl, 4 KCl, 1.5 $CaCl_2$, 1 $MgSO_4$, 0.5 Na_2HPO_4, 21 $NaHCO_3$, 30 D-glucose), and spinal cords were exposed via a ventral laminectomy and the dorsal and ventral roots cut. The spinal cord was removed, transferred to a recording chamber, ventral side up, with recirculating carbogenated aCSF at a flow rate of 20 mL/min and gradually heated from room temperature to 27º Celsius. This temperature has been used historically by our group and can control for temperature variability when experiments are conducted at room temperature. The spinal cord was allowed another 45-60 minutes to stabilize in the recording chamber.

Electrophysiological recordings

Neurograms obtained from ventral roots of the lumbar (L) 2 segments (L2), and the L5 were amplified (Dagan EX-4, 1000 times), band-pass filtered (0.1 - 1 kHz), digitized (Digidata 1440, Molecular Devices, Sunnyvale, CA), acquired (2.5 kHz) using Clampex software (Molecular Devices, Sunnyvale, CA) and saved for offline analysis. Recorded motor activity was analyzed using custom-written Matlab scripts, Spike2 (Cambridge Electronics, Cambridge, UK) and Spinal Core (Mor and Lev-Tov, 2007).

Pharmacology

Patterns of rhythmic motor activity were evoked by bath application of dopamine hydrochloride (Sigma-Aldrich, Oakville, ON, Canada) or serotonin (5-HT) hydrochloride (Sigma-Aldrich). Spinal motor network excitability was manipulated pharmacologically by altering the concentration of KCl (VWR, Edmonton, AB, Canada) in the bath, applying concentrations of NMDA (2-6 µM; Sigma-Aldrich) sub-threshold to those that are capable of evoking locomotor patterns of activity in our hands (10-12 µM), and concentrations of $MgSO_4$ (1.0-2.5 mM; VWR) to reduce but not suppress all network activity. The NMDA receptor antagonist DL-2-Amino-5-phosphonopentanoic acid (APV) was also bath-applied at concentrations capable of reducing but not suppressing spontaneous activity (5 µM; Tocris Bioscience, Bristol, UK).

Data Analysis

Patterns of rhythmic motor activity were analyzed by performing a Morlet cross wavelet analysis on ventral root recordings made from left and right L2 and L5 spinal segments and ipsilateral L2-L5 pairs (Mor and Lev-Tov, 2007). Autowavelet spectral analysis was conducted on single ventral root recordings for dopamine dose-response experiments. Spectrograms are displayed with a white V-shaped cone of influence. Frequency-power spectrograms were constructed and data analyzed by selecting regions of interest within the cone of influence. The spectrograms illustrate two distinct rhythms evoked by dopamine at high concentrations - a slow rhythm of 0.01-0.04 Hz and a fast rhythm at 0.8-1.2 Hz (e.g. Figure 1B). Regions of interest were selected within these frequency ranges and analyzed over the time course of each experiment. Parameters measured within each region of interest include frequency and power. Circular statistics were also examined to explore aspects of the pattern of bursting between neurograms recorded from root pairs (i.e. alternating: 180 degrees or synchronous: 0/360 degrees) and include the phase relationship (vector angle) between bursts in the left and right or L2-L5 roots and phase vector length (r). Data analyzed within regions of interest over the course of each experiment were segmented into 30 s bins and further averaged over 5 minute intervals for statistical analysis. All

152 analyses conducted on rhythmic motor activity were conducted using the data analysis tools available in
153 Spinal Core (Mor and Lev-Tov, 2007).

154 *Statistics*

155 Repeated measures ANOVAs were conducted for experiments that involved manipulation of network
156 excitation state after the addition of dopamine (i.e. KCl or NMDA). Tukey post hoc analyses were
157 conducted when significant main effects were detected with $p<0.05$. One way ANOVAs were performed
158 for excitability reduction experiments. Post hoc analyses were performed comparing frequency power
159 for each experiment to frequency power of rhythms evoked by 50 µM dopamine alone in previous
160 experiments. Non-parametric Friedman repeated measures ANOVA or Mann Whitney Rank Sum tests
161 were conducted when assumptions of normality or equal variance were violated using a Shapiro-Wilk
162 test and Brown-Forsythe test respectively. Power analyses could not be conducted on non-parametric
163 statistics.

164 **Results**

165 *Dopamine evokes multiple patterns of rhythmic motor activity*

166 We first examined the rhythmic activity evoked by dopamine alone – a neuromodulator often used to
167 modulate locomotor activity (Barriere et al., 2004, Bonnot et al., 2002, Whelan et al., 2000, Humphreys
168 and Whelan, 2012, Sharples et al., 2015, Picton et al., 2016). The rhythm that emerged following bath
169 application of 50 µM dopamine does not resemble a fictive locomotor pattern which is typically
170 characterized by continuous and alternating bursts between left and right sides within segments and
171 alternation between ipsilateral L2 and L5 bursts. Instead, the rhythm evoked by dopamine consists of a
172 slow and a fast component. The slow episodes occurred synchronously across left and right ventral roots
173 in the L2 (phase: 20.5 degrees, $r = 0.89$, $p < 0.0001$) and L5 (phase: 16.4 degrees, $r = 0.87$, $p < 0.0001$)
174 (Figure 1A & Ei) and between ipsilateral ventral root bursts in the L2 and L5 (phase: 14.0 degrees, r =

0.91, $p < 0.0001$). The bouts had a cycle period of 50 ± 15 s (Figure 1Di) with the onset phase locked across L2 and L5 bursts. Episode durations are significantly longer in L2 segments compared to L5's possibly reflecting a rostrocaudal gradient of excitability for dopamine (Christie and Whelan, 2005) (Figure 1Dii: L2: 30.5 ± 19 s; L5: 23.0 ± 7.9 s; Wilcoxon Signed Rank test: W = -160, T+ = 25, T- = -185, Z = -2.99, p = 0.002). The slow rhythm can be observed in the high power region within the frequency-power spectrogram around 0.02 Hz (Figure 1C).

The slow depolarizing episodes activated a faster rhythm which was superimposed on the episodes and is illustrated in the fast rhythm band in Figure 1B. In both the L2's and the L5's the fast rhythm slows from 1.1 ± 0.3 Hz to 0.83 ± 0.2 Hz over the course of the episode (Figure 1Diii; L2: $t_{(18)} = 4.9$, $p < 0.00006$; L5: $t_{(18)} = 4.9$, $p = 0.00005$) with no change in rhythm power over the course of an episode and no difference in power between L2 and L5 segments (Figure 1 Div.). We found instances when the pattern of bursts between ventral root neurograms of left and right L2, left and right L5 or ipsilateral L2-L5 pairs within the fast rhythm start off synchronous and switched to an alternating pattern toward the end of the episode (i.e. Figure 1Eii). There are also episodes where the fast rhythm is either alternating or synchronous between root pairs for the duration of the episode. Of note, the pattern never started off alternating and changed to synchrony. Examination of the fast rhythm in all episodes in the left and right L2 neurograms revealed that the predominant pattern consists of a fast rhythm that starts off alternating and finishes alternating (54.5 % of episodes). This is in contrast to the predominant pattern of bursting between ipsilateral L2 and L5 & left-right L5 which start off synchronous and ended synchronous (iL2-L5: 51.8 % of bursts; L-R L5: 85.8 % of episodes) (Figure 1Eiii). The predominant burst pattern within each ventral root pair is reflected in the mean vector plots when the data from all episodes are averaged as the average pattern is alternating within the L2s (Figure 1Fi; phase: 154.4 degrees, r = 0.65, Raleigh p = 0.0001), synchronous in the L5s (phase: 20.3 degrees, r = 0.72, Raleigh p =

198 0.00002) and biased toward synchrony in the ipsilateral L2-L5s (Figure 1Fii; phase: 78.6 degrees, r = 0.45,
199 p = 0.02).

200 Different patterns of rhythmic motor activity were expressed at different concentrations of dopamine
201 tested in a series of experiments (Figure 2). Recording from single L2 ventral roots, we determined that
202 30 µM was the lowest concentration of dopamine capable of evoking rhythmicity in 5/8 preparations.
203 100 µM evoked robust discontinuous multi-rhythmic activity (7/9) or even weak continuous rhythmicity
204 (2/9) and 300 µM evoked robust continuous patterns of rhythmicity (6/8 preps). In rhythmic
205 preparations, the time from the addition of dopamine until the first bout of rhythmicity decreased as a
206 function of dopamine concentration (30 µM = 562 ± 173 s; 100 µM = 338 ± 70 s; 300 µM = 231 ± 46 s;
207 $H(2) = 14.4$, $p < 0.001$). The frequency of the fast rhythm was significantly higher at 30 µM compared to
208 100 and 300 µM (Figure 2Ci, $F_{(2,19)} = 186$, $p < 0.001$). The fast rhythm slowed down and became more
209 robust (greater power) as a function of dopamine concentration (Figure 2Cii, $F_{(2,19)} = 20.33$, $p < 0.001$) as
210 the rhythm switched from a multi-rhythm at 100 µM to a continuous rhythm at 300 µM.

211 *Dopamine-evoked rhythmicity is dependent on network excitation state*

212 The position of the network within parameter state space has been proposed to affect how
213 neuromodulators influence rhythmic motor network output (Marder et al., 2014) and may contribute to
214 the variability we observed with respect to the diversity in rhythmic patterns evoked at different
215 dopamine concentrations. Conceptually, if a neuromodulator is acting around the transition point for a
216 network, where the pattern would change, a similar change in intrinsic properties of a class of neurons
217 within the network would have a large effect compared to when it operates far from the transition
218 borders. We therefore devised a series of experiments whereby the global excitability of spinal motor
219 networks was manipulated by increasing the concentration of extracellular KCl in the bath or by

application of NMDA to non-specifically excite spinal motor networks. The goal here was to move the spinal network around a state-space so that we would abut transition zones.

Following bath application of 50 µM of dopamine and generation of a regular multi-rhythm, bath KCl concentration was sequentially increased from basal levels (4 mM KCl in the aCSF) in 2 mM increments and the resultant effects on the rhythm was recorded (Figure 3; n =10). The duration of the episodes that composed the slow rhythm decreased as KCl was increased and differences in episode duration in L2 and L5 were no longer apparent at 6 and 8 mM KCl (Baseline: L2: 31±26 s, L5: 23.6±9.5 s; 6mM: L2: 17.7± 5 s, L5: 15.0s ± 2.5 s; 8 mM: L2: 12.4 ± 2.4 s, L5: 11.8 ± 2.3 s). Boosting network excitation via KCl decreased the frequency of the fast rhythm (L2: $F_{(11,99)} = 5.9$, $p < 0.001$; L5: $F_{(11, 88)} = 0.47$, $p = 0.9$) and increased the frequency of the slow rhythm (L2: $F_{(11, 99)} = 3.7$, $p < 0.001$) in the L2s. The power of the fast rhythm increased (L2: $X^2_{(11)} = 53.7$, $p < 0.001$; L5: $\chi^2_{(11)} = 51.2$, $p < 0.001$) and slow rhythm decreased (L2: $\chi^2_{(11)} = 63.8$, $p < 0.001$; L5: $F_{(10,80)} = 8.3$, $p<0.001$) in both the L2's and L5's (Figure 3Di & Dii) as excitation was increased and is a reflection of the rhythm switching from discontinuous multi-rhythm to a continuous rhythm. The pattern of the fast rhythm became more locomotor-like as excitation was increased indicated by the phase moving toward 180 degrees in the left and right L2's (Figure 3Ei), ipsilateral L2 and L5 (Figure 3Eii) and left and right L5's (DA baseline: phase: 13.5 degrees, r= 0.75, p = 0.004; 10 mM KCl: phase: 145 degrees, r = 0.43, p = 0.2).

These effects were replicated when network excitation was enhanced by addition of 10 mM KCl prior to application of 50 µM of dopamine (Figure 4Di & Dii; n = 7 L2 Power: fast rhythm: $F_{(1,100)} = 7.4$, p= 0.008; Slow rhythm: $F_{(1,100)} = 33.6$, $p < 0.0001$). No rhythmicity was observed at 10 mM KCl alone; however, addition of 50 µM dopamine evoked a continuous locomotor-like rhythm with alternation in the left and right L2 and L5, and ipsilateral L2-L5, with no transition through a multi-rhythmic pattern (Figure 4Ei & Eii: L2-L2 phase: 170 degrees, r = 0.91, Raleigh p = 0.0009; L5-L5 phase: 157 degrees, r = 0.72, Raleigh p = 0.02, iL2-L5: phase: 146 degrees, r = 0.95, p=0.0003). This reverted back to a multi-rhythm with a wash

in of 50 µM of dopamine with regular (4 mM KCl) aCSF with no significant difference in fast or slow rhythm power under the wash conditions compared to the expected basal rhythm power (Figure 4Di & Dii; n = 5 L2 Power: fast rhythm: $F_{(1,92)} = 1.3$, $p = 0.25$; Slow rhythm: $F_{(1,92)} = 0.78$, $p = 0.4$). These data indicate that there were no significant order effects due to sequential administration of KCl or second-messenger desensitization effects with time.

In a complimentary set of experiments, following the generation of a robust multi-rhythm, network excitation was reduced by washing in 50 µM of dopamine in aCSF with 1 mM KCl (Figure 5A). As expected, the power of the fast rhythm degraded in the L2's (Figure 5Fi; n = 6, $p = 0.02$) and a trend toward reduced power the L5's (Figure 5Fii, n = 5; $p= 0.06$) with no significant reduction in the slow rhythm (Figure 5Fiii & Fiv). Similarly, 50 µM of dopamine had a qualitatively smaller effect on network dynamics when it was presumably far from a transition point, as it did not evoke a fast rhythm when preparations were recovered in aCSF with 1 mM KCl for 1 hour prior to dopamine application (Figure 5B & Fi-Fii: L2: $p < 0.001$; L5: $p = 0.004$). In both experiments, the rhythm was slightly recovered by washing in regular aCSF (4 mM KCl) (Figure 5A & B).

Manipulating the extracellular KCl concentration also affects chloride concentrations. We reproduced the above experiments using NMDA to increase excitability across neuronal populations using concentrations (2 - 6 µM) subthreshold to those that evoke rhythmicity on their own (Figure 6; n = 10). The duration of the episodes that compose the slow rhythm decreased as NMDA was increased and differences in episode duration in L2 and L5 were no longer apparent at 2 and 4 µM NMDA (Baseline: L2: 29 ± 9.5 s, L5: 22.6 ± 6.5 s; 2 µM: L2: 19.4 ± 7 s, L5: 17.2 s ± 4.1 s; 4 µM: L2: 13.2 ± 4.3 s, L5: 12.6 ± 4.5 s). Boosting network excitation via NMDA decreased the frequency of the fast rhythm (L2: $\chi^2_{(11)} = 64.3$, $p < 0.001$; L5: $F_{(11, 99)} = 8.8$, $p < 0.001$) and increased the frequency of the slow rhythm (L2: $\chi^2_{(11)} = 22.2$, $p < 0.05$; L5: $F_{(11, 99)} = 18.2$, $p < 0.001$) in the L2's and the L5's. The power of the fast rhythm increased

(Figure 6Di: L2: $X^2_{(11)} = 82.7$, $p < 0.001$; L5: $F_{(11, 99)} = 12.1$, $p < 0.001$) and slow rhythm decreased in both the L2's and L5's (Figure 6Dii: L2: $\chi^2_{(11)} = 66.7$, $p < 0.001$; L5: $\chi^2_{(11)} = 46.6$, $p < 0.001$) as excitation was increased reflecting the rhythm switching from discontinuous multi-rhythm to a continuous rhythm. Likewise, the pattern of the fast rhythm became more locomotor-like as indicated by an increase in the mean vector length (r) pointing toward 180 degrees (alternating) in the left and right L2's (Figure 6Ei) ipsilateral L2 and L5 (Figure 6Eii) and left and right L5's (DA baseline: L5-L5 phase: 16.1 degrees, $r = -0.7$, $p = 0.005$; 6 µM NMDA: L5-L5 phase: 113 degrees, $r = 0.42$, $p = 0.2$).

In an additional set of experiments, during rhythmic activity evoked by dopamine, network excitation was progressively reduced by incrementally increasing the concentration of Mg^{2+} in the bath ($MgSO_4$). Increasing extracellular Mg^{2+} reduces the efficacy of NMDA-mediated synaptic transmission that is necessary for rhythmogenesis in the spinal cord (Soffe and Roberts, 1989) by impairing the removal of the voltage-dependent Mg^{2+} block in the NMDA channel. This manipulation was thus used as a means of reducing global network excitation by reducing the efficacy of excitatory synaptic transmission. Sequential increase in Mg^{2+} from basal levels (1.0 mM) to 1.5 mM progressively degraded the multi-rhythm and fully disrupted rhythmic activity at 2.0 mM as reflected in significant reduction in power of the both the fast rhythm (Figure 5C & Fi-Fii, n = 6, L2: $p < 0.001$; L5: $p < 0.001$) and slow rhythm (Figure 5 Fiii-Fiv, n = 6, L2: $p < 0.001$; L5: $p < 0.001$) in both the L2's and L5's. Subsequent experiments where NMDA channels were antagonized with a low concentration of APV (5 µM) also inhibited the fast (n = 6, $p < 0.001$) and slow rhythm (n = 6, $p = 0.03$) in the L2's but not the fast rhythm (Figure 5D & Fi-Fii, n = 6, $p= 0.1$) or slow rhythm (Figure 5D & Fiii-Fiv, n = 6, $p = 0.7$) in the L5's.

5-HT-evoked rhythmicity is also influenced by network excitation

The above experiments describe how network excitation state influences dopamine's modulatory effect on spinal motor output. Multi-rhythmic patterns of motor activity have been reported to be generated

by a number of modulators including noradrenaline, trace amines (Gozal et al., 2014), and 5-HT (MacLean et al., 1998, Schmidt et al., 1998). We next examined the generalizability of state-dependency using 5-HT instead of dopamine. Examination of the frequency power spectrum over time following application of low concentrations of 5-HT reveals that it too, although qualitatively different than dopamine, exhibits a slow underlying rhythm that is most apparent in the L2's and disappears as the concentration is increased (Figure 7A). If this slow rhythm is a network phenomenon that is expressed at intermediate levels of excitation, then it should disappear as network excitation increases. To test this hypothesis, we sequentially increased network excitation in 2 mM KCl increments following the application of 15 µM 5-HT which was the most effective at evoking both slow and fast rhythms simultaneously. As expected, KCl increased the robustness of the fast, locomotor-like rhythm (Figure 7Di: n = 5 L2: $F_{(4,43)} = 5.2$, $p < 0.001$; L5: $F_{(4,44)} = 13.9$, $p < 0.001$) and decreased the power of the slow rhythm (Figure 7Dii: n = 5 L2: $F_{(4,43)} = 4.6$, $p < 0.001$; L5: $X^2_{(11)} = 31.1$, $p < 0.001$) up to 8 mM of KCl, with 10 mM causing a shift to tonic activity and resultant decline in power of both the fast and slow rhythms (Figure 7Di-Dii).

Discussion

Neuromodulators play a critical role in sculpting network behavior but these effects are state-dependent (Marder et al., 2014). We made use of a well-defined mouse model to explore how network excitation state dictates the modulatory effects of dopamine on spinal locomotor circuits. When we moved the excitation state of the network we found four stable zones where dopamine produced discrete network behaviors (Figure 8). While dopamine was used here, our work suggests that these findings are relevant to other modulators such as serotonin and this generalizability has been pointed out in invertebrate systems (Gutierrez et al., 2013, Marder et al., 2014). Our work provides an understanding into variability in modulatory action between preparations which is a common challenge when studying network

function *in vitro*. These results have important implications with respect to the effect of manipulations on cellular elements of the network that may move the network across state space.

Motor networks of the lumbar spinal cord are capable of generating a diverse array of rhythmic motor patterns including locomotion, scratching, spontaneous activity and other movements. Most studies exploring modulation of rhythms *in vitro* focus on a continuous locomotor-like rhythms (Brownstone and Wilson, 2008, Hagglund et al., 2013, Kiehn and Kjaerulff, 1996, Kiehn et al., 1999, Madriaga et al., 2004, Pearlstein et al., 2005) which coincide with state 4 in Figure 8. While different labs use varying concentrations of NMDA, 5-HT or dopamine to elicit rhythmic activity (Whelan et al., 2000, Bonnot et al., 2002, Madriaga et al., 2004, Sharples et al., 2015, Cazalets et al., 1992, Zhong et al., 2010, Zhong et al., 2011), what is of note is that once state 4 is reached it is characterized by stable alternating bursting. Indeed, there are subtle differences in the rhythms published by various labs, what is perhaps most striking are the similarities in fictive-locomotor patterns. One possibility could be that subtle modulatory effects may be less apparent during a high conductance state (Berg et al., 2007). Previous work conducted by our lab utilized an unstable, locomotor rhythm generated at the lower excitation region of state 4 to reveal the stabilizing effect of dopamine (Sharples et al., 2015). Others have shown a similar effect of oxytocin (Dose et al., 2014, Pearson et al., 2003). A revised interpretation of our previous findings in light of our recent data is illustrated in Figure 9. An important caveat is that our data examines a network in a state of development. We have interpreted this based on such a network and recognize that the adult network likely responds differently and that receptor densities and functional effects are known to change during development (Perrier and Hounsgaard, 2000, Picton and Sillar, 2016, Clemens et al., 2012, Keeler et al., 2016).

Dopamine reveals state-dependent recruitment of spinally-generated rhythmicity

335 In the current work, the rhythmogenic effects of dopamine were dependent on excitation state of the
336 spinal cord. In particular, we demonstrate that manipulating network excitation can reproduce the same
337 network output that we report only at high concentrations of dopamine. We replicated this finding using
338 several complimentary non-specific methods to manipulate network excitation including increasing
339 extracellular KCl and NMDA to increase excitation and low KCl, Mg^{2+} and APV to reduce network
340 excitation. Our work does not suggest that neuromodulator action is wholly dependent on network
341 excitability as modulators have network effects beyond solely increasing network excitation. For
342 example, we found that 5-HT can evoke rhythms that are qualitatively different from dopamine's, but
343 notably we found that the rhythms produced by 5-HT are also dependent on excitation state. Indeed,
344 simply altering the extracellular ionic composition of potassium and calcium is sufficient in itself to drive
345 rhythmicity at the network and interneuronal level through the recruitment of voltage-sensitive sodium
346 persistent inward currents (Brocard et al., 2013).

347 In other states the situation is more complex. We found that the rhythm evoked by our initial
348 concentration of dopamine used to modulate locomotion (Whelan et al., 2000, Jiang et al., 1999) does
349 not resemble the rhythmic signature typically associated with walking. While the episodes of rhythmicity
350 were regular, the phasing of the intra-episode fast rhythm between roots was less stable. Upon initial
351 observation one could conclude that this is the discrete rhythmic motor pattern evoked by dopamine.
352 Others have explored rhythms which transit between states 1 and 3 (Figure 8), and inferred discrete
353 modulatory function (Cazalets et al., 1992, Gozal et al., 2014, Pearson et al., 2003, Schmidt et al., 1998).
354 It could therefore be argued that this multi-rhythmic pattern of activity may be a more non-physiological
355 motor pattern occupying state 3 and expressed under the lower levels of excitation present in reduced
356 preparations of the nervous system.

357 On the other hand, neonatal rodent pups move towards the dam to suckle and move towards their litter
358 mates to keep warm. While neonates do not fully bear their weight or produce functional walking

359 movements, they do produce a diverse array of rhythmic movements of the limbs that allow them to
360 move around the nest. Although speculative, our work could be a representation of these diverse
361 patterns that are expressed as networks enter transition zones during development. As descending
362 pathways mature and excitability of spinal networks becomes more robust, stable locomotor patterns
363 similar to state 4 would begin to emerge. Similar to developing systems, pathological rhythmic motor
364 patterns could also emerge in adults when spinal networks move into a lower excitation state due to
365 impaired descending activation of spinal motor networks. In other systems, such as epilepsy, altered
366 excitation states can produce slow rhythms similar to what we have observed, but any mechanistic
367 similarities remain speculative at this point (Jensen and Yaari, 1997).

368 Finally, state 1, or the basal state, in the neonatal rodent spinal cord is characterized by spontaneous
369 activity. An interesting feature of spontaneous activity comes from previous work on the mouse where
370 multiple rhythmic patterns were observed, from high frequency synchronous bursts, to ipsilateral
371 bursting, and locomotor-like activity (Whelan et al., 2000). A hypothesis would then form that several
372 transient states exist that converge onto a fourth locomotor-like state. We suspect that dopamine may
373 be accessing a portion of these transient states and forming several identifiable and stable states. As to
374 how dopamine can excite the cord forming regular episodes of rhythmic activity in state 3, compared to
375 stochastic activation with spontaneous bursting activity in state 1 is unclear.

376 *Implications and Summary*

377 Our work illustrates at least four definable network states which restrict the effects that a
378 neuromodulator can elicit within the lumbar spinal cord (Figure 8). For example, the effects of dopamine
379 on a stable locomotor-like pattern are arguably rather subtle – it does reduce the frequency and
380 increases the amplitude of activity – but the rhythmic pattern remains qualitatively similar. This is very
381 different if the network is transiting to state 4 – here dopamine has a large impact on network function

382 – bursting becomes much more regular and phasing between neurograms becomes locomotor-like
383 (Sharples et al., 2015). These effects are illustrated in Figure 9. We emphasize the importance of
384 network excitation state when studying the contributions of identifiable cell types to the production of
385 spinally-generated rhythmic activity. Removal of elements that compose the CPG may move the
386 network into lower (or higher) regions of network state space. Caution is therefore advised on inferring
387 neuronal sub-type function based on altered patterns of motor activity before moving the network
388 through the full range of excitation state space. This leads us to propose that an important control
389 would be to move the network excitability in the opposite direction as the hypothesized movement of
390 the modulator. This would allow one to detail the contribution of circuit manipulation across defined
391 network states.

392

393

References

BAGHDADWALA, M. I., DUCHCHERER, M., TRASK, W. M., GRAY, P. A. & WILSON, R. J. 2016. Diving into the mammalian swamp of respiratory rhythm generation with the bullfrog. *Respir Physiol Neurobiol,* 224**,** 37-51.

BARGMANN, C. I. 2012. Beyond the connectome: how neuromodulators shape neural circuits. *Bioessays,* 34**,** 458-65.

BARRIERE, G., BERTRAND, S. & CAZALETS, J. R. 2005. Peptidergic neuromodulation of the lumbar locomotor network in the neonatal rat spinal cord. *Peptides,* 26**,** 277-86.

BARRIERE, G., MELLEN, N. & CAZALETS, J. R. 2004. Neuromodulation of the locomotor network by dopamine in the isolated spinal cord of newborn rat. *Eur J Neurosci,* 19**,** 1325-35.

BERG, R. W., ALABURDA, A. & HOUNSGAARD, J. 2007. Balanced inhibition and excitation drive spike activity in spinal half-centers. *Science,* 315**,** 390-3.

BLITZ, D. M. & NUSBAUM, M. P. 2012. Modulation of circuit feedback specifies motor circuit output. *J Neurosci,* 32**,** 9182-93.

BONNOT, A., WHELAN, P. J., MENTIS, G. Z. & O'DONOVAN, M. J. 2002. Locomotor-like activity generated by the neonatal mouse spinal cord. *Brain Res Brain Res Rev,* 40**,** 141-51.

BOUVIER, J., CAGGIANO, V., LEIRAS, R., CALDEIRA, V., BELLARDITA, C., BALUEVA, K., FUCHS, A. & KIEHN, O. 2015. Descending Command Neurons in the Brainstem that Halt Locomotion. *Cell,* 163**,** 1191-203.

BROCARD, F., SHEVTSOVA, N. A., BOUHADFANE, M., TAZERART, S., HEINEMANN, U., RYBAK, I. A. & VINAY, L. 2013. Activity-dependent changes in extracellular Ca2+ and K+ reveal pacemakers in the spinal locomotor-related network. *Neuron,* 77**,** 1047-54.

BROWNSTONE, R. M. & WILSON, J. M. 2008. Strategies for delineating spinal locomotor rhythm-generating networks and the possible role of Hb9 interneurones in rhythmogenesis. *Brain Res Rev,* 57**,** 64-76.

CAZALETS, J. R., SQALLI-HOUSSAINI, Y. & CLARAC, F. 1992. Activation of the central pattern generators for locomotion by serotonin and excitatory amino acids in neonatal rat. *J Physiol,* 455**,** 187-204.

CHRISTIE, K. J. & WHELAN, P. J. 2005. Monoaminergic establishment of rostrocaudal gradients of rhythmicity in the neonatal mouse spinal cord. *J Neurophysiol,* 94**,** 1554-64.

CLEMENS, S., BELIN-RAUSCENT, A., SIMMERS, J. & COMBES, D. 2012. Opposing modulatory effects of D1- and D2-like receptor activation on a spinal central pattern generator. *J Neurophysiol,* 107**,** 2250-9.

COWLEY, K. C. & SCHMIDT, B. J. 1997. Regional distribution of the locomotor pattern-generating network in the neonatal rat spinal cord. *J Neurophysiol,* 77**,** 247-59.

DOSE, F., ZANON, P., COSLOVICH, T. & TACCOLA, G. 2014. Nanomolar oxytocin synergizes with weak electrical afferent stimulation to activate the locomotor CpG of the rat spinal cord in vitro. *PLoS One,* 9**,** e92967.

GORDON, I. T. & WHELAN, P. J. 2006. Monoaminergic control of cauda-equina-evoked locomotion in the neonatal mouse spinal cord. *J Neurophysiol,* 96**,** 3122-9.

GOZAL, E. A., O'NEILL, B. E., SAWCHUK, M. A., ZHU, H., HALDER, M., CHOU, C. C. & HOCHMAN, S. 2014. Anatomical and functional evidence for trace amines as unique modulators of locomotor function in the mammalian spinal cord. *Front Neural Circuits,* 8**,** 134.

GRILLNER, S., WALLEN, P., SAITOH, K., KOZLOV, A. & ROBERTSON, B. 2008. Neural bases of goal-directed locomotion in vertebrates--an overview. *Brain Res Rev,* 57**,** 2-12.

GUTIERREZ, G. J. & MARDER, E. 2014. Modulation of a Single Neuron Has State-Dependent Actions on Circuit Dynamics. *eNeuro,* 1.

GUTIERREZ, G. J., O'LEARY, T. & MARDER, E. 2013. Multiple mechanisms switch an electrically coupled, synaptically inhibited neuron between competing rhythmic oscillators. *Neuron,* 77**,** 845-58.

HAGGLUND, M., DOUGHERTY, K. J., BORGIUS, L., ITOHARA, S., IWASATO, T. & KIEHN, O. 2013. Optogenetic dissection reveals multiple rhythmogenic modules underlying locomotion. *Proc Natl Acad Sci U S A,* 110**,** 11589-94.

HECKMAN, C. J. & JOHNSON, M. D. 2014. Reconfiguration of the electrical properties of motoneurons to match the diverse demands of motor behavior. *Adv Exp Med Biol,* 826**,** 33-40.

HENTALL, I. D., MESIGIL, R., PINZON, A. & NOGA, B. R. 2003. Temporal and spatial profiles of pontine-evoked monoamine release in the rat's spinal cord. *J Neurophysiol,* 89**,** 2943-51.

HULTBORN, H. & NIELSEN, J. B. 2007. Spinal control of locomotion--from cat to man. *Acta Physiol (Oxf),* 189**,** 111-21.

HUMPHREYS, J. M. & WHELAN, P. J. 2012. Dopamine exerts activation-dependent modulation of spinal locomotor circuits in the neonatal mouse. *J Neurophysiol,* 108**,** 3370-81.

JENSEN, M. S. & YAARI, Y. 1997. Role of intrinsic burst firing, potassium accumulation, and electrical coupling in the elevated potassium model of hippocampal epilepsy. *J Neurophysiol,* 77**,** 1224-33.

JIANG, Z., CARLIN, K. P. & BROWNSTONE, R. M. 1999. An in vitro functionally mature mouse spinal cord preparation for the study of spinal motor networks. *Brain Res,* 816**,** 493-9.

JORDAN, L. M., LIU, J., HEDLUND, P. B., AKAY, T. & PEARSON, K. G. 2008. Descending command systems for the initiation of locomotion in mammals. *Brain Res Rev,* 57**,** 183-91.

KEELER, B. E., LALLEMAND, P., PATEL, M. M., DE CASTRO BRAS, L. E. & CLEMENS, S. 2016. Opposing aging-related shift of excitatory dopamine D1 and inhibitory D3 receptor protein expression in striatum and spinal cord. *J Neurophysiol,* 115**,** 363-9.

KIEHN, O. 2016. Decoding the organization of spinal circuits that control locomotion. *Nat Rev Neurosci,* 17**,** 224-38.

KIEHN, O. & KJAERULFF, O. 1996. Spatiotemporal characteristics of 5-HT and dopamine-induced rhythmic hindlimb activity in the in vitro neonatal rat. *J Neurophysiol,* 75**,** 1472-82.

KIEHN, O., SILLAR, K. T., KJAERULFF, O. & MCDEARMID, J. R. 1999. Effects of noradrenaline on locomotor rhythm-generating networks in the isolated neonatal rat spinal cord. *J Neurophysiol,* 82**,** 741-6.

KIMURA, Y., SATOU, C., FUJIOKA, S., SHOJI, W., UMEDA, K., ISHIZUKA, T., YAWO, H. & HIGASHIJIMA, S. 2013. Hindbrain V2a neurons in the excitation of spinal locomotor circuits during zebrafish swimming. *Curr Biol,* 23**,** 843-9.

KOBLINGER, K., FUZESI, T., EJDRYGIEWICZ, J., KRAJACIC, A., BAINS, J. S. & WHELAN, P. J. 2014. Characterization of A11 neurons projecting to the spinal cord of mice. *PLoS One,* 9**,** e109636.

MACLEAN, J. N., COWLEY, K. C. & SCHMIDT, B. J. 1998. NMDA receptor-mediated oscillatory activity in the neonatal rat spinal cord is serotonin dependent. *J Neurophysiol,* 79**,** 2804-8.

MADRIAGA, M. A., MCPHEE, L. C., CHERSA, T., CHRISTIE, K. J. & WHELAN, P. J. 2004. Modulation of locomotor activity by multiple 5-HT and dopaminergic receptor subtypes in the neonatal mouse spinal cord. *J Neurophysiol,* 92**,** 1566-76.

MARDER, E., GOERITZ, M. L. & OTOPALIK, A. G. 2015. Robust circuit rhythms in small circuits arise from variable circuit components and mechanisms. *Curr Opin Neurobiol,* 31**,** 156-63.

MARDER, E., O'LEARY, T. & SHRUTI, S. 2014. Neuromodulation of circuits with variable parameters: single neurons and small circuits reveal principles of state-dependent and robust neuromodulation. *Annu Rev Neurosci,* 37**,** 329-46.

MILES, G. B. & SILLAR, K. T. 2011. Neuromodulation of vertebrate locomotor control networks. *Physiology (Bethesda),* 26**,** 393-411.

MOR, Y. & LEV-TOV, A. 2007. Analysis of rhythmic patterns produced by spinal neural networks. *J Neurophysiol,* 98**,** 2807-17.

PEARLSTEIN, E., BEN MABROUK, F., PFLIEGER, J. F. & VINAY, L. 2005. Serotonin refines the locomotor-related alternations in the in vitro neonatal rat spinal cord. *Eur J Neurosci,* 21**,** 1338-46.

PEARSON, S. A., MOUIHATE, A., PITTMAN, Q. J. & WHELAN, P. J. 2003. Peptidergic activation of locomotor pattern generators in the neonatal spinal cord. *J Neurosci,* 23**,** 10154-63.

PERRIER, J. F. & HOUNSGAARD, J. 2000. Development and regulation of response properties in spinal cord motoneurons. *Brain Res Bull,* 53**,** 529-35.

PICTON, L. D., NASCIMENTO, F., BROADHEAD, M. J., SILLAR, K. T. & MILES, G. B. 2016. Sodium pumps mediate activity-dependent changes in mammalian motor networks. *J Neurosci*.

PICTON, L. D. & SILLAR, K. T. 2016. Mechanisms underlying the endogenous dopaminergic inhibition of spinal locomotor circuit function in Xenopus tadpoles. *Sci Rep,* 6**,** 35749.

PRINZ, A. A., BUCHER, D. & MARDER, E. 2004. Similar network activity from disparate circuit parameters. *Nat Neurosci,* 7**,** 1345-52.

PUHL, J. G. & MESCE, K. A. 2008. Dopamine activates the motor pattern for crawling in the medicinal leech. *J Neurosci,* 28**,** 4192-200.

ROBERTS, A., LI, W. C. & SOFFE, S. R. 2012. A functional scaffold of CNS neurons for the vertebrates: the developing Xenopus laevis spinal cord. *Dev Neurobiol,* 72**,** 575-84.

SCHMIDT, B. J., HOCHMAN, S. & MACLEAN, J. N. 1998. NMDA receptor-mediated oscillatory properties: potential role in rhythm generation in the mammalian spinal cord. *Ann N Y Acad Sci,* 860**,** 189-202.

SHARPLES, S.A. & WHELAN, P.J. 2015. Dopamine exerts concentration-dependent bidirectional modulation and evokes state-dependent rhythmicity in motor networks of the neonatal mouse spinal cord. 422.07. *Society for Neuroscience.* Chicago, IL.

SHARPLES, S. A., HUMPHREYS, J. M., JENSEN, A. M., DHOOPAR, S., DELALOYE, N., CLEMENS, S. & WHELAN, P. J. 2015. Dopaminergic modulation of locomotor network activity in the neonatal mouse spinal cord. *J Neurophysiol,* 113**,** 2500-10.

SILLAR, K. T., COMBES, D. & SIMMERS, J. 2014. Neuromodulation in developing motor microcircuits. *Curr Opin Neurobiol,* 29**,** 73-81.

SMITH, J. C., ELLENBERGER, H. H., BALLANYI, K., RICHTER, D. W. & FELDMAN, J. L. 1991. Pre-Botzinger complex: a brainstem region that may generate respiratory rhythm in mammals. *Science,* 254**,** 726-9.

SOFFE, S. R. & ROBERTS, A. 1989. The Influence of Magnesium Ions on the NMDA Mediated Responses of Ventral Rhythmic Neurons in the Spinal Cord of Xenopus Embryos. *Eur J Neurosci,* 1**,** 507-515.

STADELE, C., HEIGELE, S. & STEIN, W. 2015. Neuromodulation to the Rescue: Compensation of Temperature-Induced Breakdown of Rhythmic Motor Patterns via Extrinsic Neuromodulatory Input. *PLoS Biol,* 13**,** e1002265.

VAN DEN POL, A. N. 1999. Hypothalamic hypocretin (orexin): robust innervation of the spinal cord. *J Neurosci,* 19**,** 3171-82.

WHELAN, P., BONNOT, A. & O'DONOVAN, M. J. 2000. Properties of rhythmic activity generated by the isolated spinal cord of the neonatal mouse. *J Neurophysiol,* 84**,** 2821-33.

WHELAN, P. J., HIEBERT, G. W. & PEARSON, K. G. 1995. Stimulation of the group I extensor afferents prolongs the stance phase in walking cats. *Exp Brain Res,* 103**,** 20-30.

ZHONG, G., DROHO, S., CRONE, S. A., DIETZ, S., KWAN, A. C., WEBB, W. W., SHARMA, K. & HARRIS-WARRICK, R. M. 2010. Electrophysiological characterization of V2a interneurons and their locomotor-related activity in the neonatal mouse spinal cord. *J Neurosci,* 30**,** 170-82.

ZHONG, G., SHARMA, K. & HARRIS-WARRICK, R. M. 2011. Frequency-dependent recruitment of V2a interneurons during fictive locomotion in the mouse spinal cord. *Nat Commun,* 2**,** 274.

Figure 1: Dopamine evokes multi-rhythmic patterns of motor activity. (A). Neurograms recorded from the left and right ventral roots of the second (L2) and fifth (L5) isolated thoraco-lumbar spinal cord. (B). Dopamine evokes a multi-rhythmic pattern of motor activity that is composed of two rhythms: a slow, synchronous rhythm with a superimposed fast rhythm. (C). These fast and slow rhythms (C - red boxes) are apparent when the frequency power is represented over time as a spectrogram with frequency on the left Y-axis, time on the X-axis and warmer colours representing higher frequency power. (D).The slow rhythm features including cycle period (Di), episode duration (Dii.), and power (Div.) did not differ between L2 (red bars) and L5 (black bars) segments. The frequency of the fast rhythm occurring within bouts (Diii.) decreases over the course of the bout (Div.) with no difference in power between L2 and L5 (Div). Data are displayed as mean ± SD. (Ei). Example phase plots from a single bout of rhythmic activity recorded from the L2 segment illustrate that the bouts are synchronous with the fast superimposed rhythm exhibiting a biphasic phase distribution. (Eii). Separating the fast rhythm into two bins illustrates that the fast bursts start off synchronous and end alternating. (Eiii). The pie charts represent the distribution of the possible patterns over the course of a bout recorded between the left and right L2 and ipsilateral L2-L5 ventral roots. (Fi). Reflects the mean phase of all bouts (Fii). The predominantly synchronous bursting pattern in ipsilateral ventral root pairs is represented in the mean phase plot. The phase in circular plots are reported in degrees with the length of arrows representing mean vector length (r) and angle.

Figure 2: High concentrations of dopamine evoke rhythmicity. (A). Neurograms from single L2 ventral roots from individual experiments with dopamine (DA) bath-applied (red arrows) at 30 µM (Ai) 100 µM (Aii) and 300 µM (Aiii) to naïve preparations evokes rhythmic motor activity. (B). The fast and slow rhythms are illustrated in the autowavelet frequency power spectrograms over time (Bi-Biii) with frequency on the left Y-axis, time on the X-axis and warmer colours representing higher power. Rhythm

frequency and power of the fast and slow rhythms were analyzed by selecting regions of interest selected within bouts of the fast rhythm and within the range of the slow rhythm. (C).The frequency of the fast rhythm slowed down (Ci) and power increased (Cii) with dopamine concentration. No differences were found in frequency (Ciii) or power (Civ) of the slow rhythm between dopamine concentrations. Data are presented as mean ± SD asterisks denoting significance (*: $p < 0.05$, **: $p < 0.01$, ***: $p < 0.001$) with Tukey post hoc following a two-way ANOVA between time (5 minute bins) and dopamine concentration.

Figure 3: Sequentially boosting network excitation with KCl modulates dopamine-evoked rhythmicity. (A). Neurograms recorded from the left and right L2 and right L5 ventral roots show raw data, and the effect on rhythmicity. Bath application of 50 µM of dopamine evokes a multi-rhythmic pattern of motor activity that is modulated as network excitation is boosted by sequentially increasing the concentration of KCl in the bath (red arrows). When KCl is increased to 10 mM, the pattern switches from multi-rhythmic, to a single, continuous locomotor-like rhythm. (B) The frequency power distribution following dopamine application and subsequent excitability manipulation is illustrated in the cross-wavelet frequency power spectrogram over time with frequency on the left Y-axis, time on the X-axis and increasing power represented as warmer colours. At 10 mM KCl, the pattern switches from multiple rhythms, to a single continuous rhythm. (C). Representative neurograms showing rhythm at baseline (Ci.), dopamine with 8 mM KCl (Cii.), and a continuous locomotor-like rhythm expressed with dopamine and 10 mM of KCl (Ciii.). (D). Regions of interest were selected around the fast and slow rhythms and respective frequency and power for left and right L2 and L5 neurograms analyzed over time. Increasing network excitation increased the power of the fast rhythm (Di) and decreased the power of the slow rhythm (Dii). Data are presented as mean ± SD with asterisks denoting a significant difference between the respective point and the rhythm at 20 minutes following dopamine application (*: $p < 0.05$, **: $p <$

582 0.01, ***: p < 0.001) obtained from Tukey post hoc analysis when significant main effects on a repeated
583 measures ANOVA were found. Non-parametric statistics were performed when assumptions of
584 normality failed and significance denoted #: p < 0.05. ##: p<0.01, ###: p < 0.001. (E). The phase between
585 L2 neurograms for the fast rhythm is presented in the circular plots in Ei and Eii and illustrate the switch
586 to a locomotor-like pattern at 10 mM KCl as the vector length increases and phase moves towards 180
587 degrees (alternating) in both the left and right L2s and ipsilateral L2-L5. Each dot represents the average
588 phase for an individual preparation for each respective experimental condition. The length of the arrows
589 represents mean vector length (r) or the robustness of the pattern.

590

591 **Figure 4: Boosting network excitation with KCl prior to application of dopamine evokes locomotor-like**
592 **rhythmicity.** (A). Neurograms recorded from left and right L2 and right L5 ventral roots illustrate the
593 experimental paradigm and resultant effect on rhythmicity. KCl concentration was increased to 10 mM
594 to boost network excitation 20 minutes prior to application of 50 µM of dopamine (DA). Subsequent
595 application of DA resulted in the direct expression of a continuous locomotor-like rhythm that returned
596 to a multi-rhythm when washed out with regular (4 mM KCl) aCSF and 50 µM of DA. (B). Frequency
597 power spectrogram with frequency on the left Y-axis, time on the X-axis and increasing power
598 represented as warmer colours. (C). Raw data showing zoomed regions represented in (B) of 50 µM
599 dopamine + 10 mM KCl (Ci), at a longer timepoint (Cii) and following wash-in of 4 mM KCl. (D). Region of
600 interest analysis of fast and slow rhythms within L2 root pairs illustrate significantly higher power of the
601 fast rhythm with 10 mM KCl compared to the expected rhythm power at 4 mM KCl (Di). The slow rhythm
602 showed significantly lower power compared to the expected multi-rhythm evoked in the 4 mM KCl
603 condition (Dii). The expected power values returned to the same level as the expected condition
604 following a wash out with 4 mM KCl (Blue lines). (E). Circular plots in Ei and Eii illustrate a locomotor-like
605 pattern with vector length increases accompanied by phase angles moving toward 180 degrees

606 (alternating) in both the left and right L2s and ipsilateral L2-L5 at higher KCl concentrations. The length
607 of arrows represents mean vector length (r) and angle or robustness of the pattern. Red lines represent
608 mean data (n=20 preparations) when 50 µM of DA (aCSF: 4 mM KCl) was applied and 20 minutes of
609 baseline data were analyzed. Black lines represent the rhythm evoked by 50 µM DA under enhanced
610 network excitation (aCSF: 10 mM KCl) and blue lines represent the wash out condition of DA (aCSF: 4
611 mM KCl). Each dot in the phase plots represents the average phase for an individual preparation for
612 each respective experimental condition. Data are presented as mean ± SD. A two-way ANOVA between
613 each excitability condition (DA-evoked rhythm in 4 mM KCl, 10 mM KCl and wash with 4 mM KCl) and
614 time to examine the effects of manipulating network excitation prior to DA application. When significant
615 main effects of interactions were detected Tukey post hoc analysis between time-matched points
616 following DA application were conducted. Asterisks denote significance with *: $p < 0.05$, **: $p < 0.01$,
617 ***: $p < 0.001$.

618 **Figure 5: Decreasing network excitation disrupts the ability of dopamine to evoke rhythmicity.** (A-D).
619 Neurograms from single ventral roots within the L5 illustrate the overall effect of reducing network
620 excitation via several pharmacological approaches on dopamine-evoked rhythmicity. (A). In the first
621 experiment, network excitability was reduced by washing in aCSF containing 1 mM KCl after evoking a
622 rhythm, (B). In a second experiment, preparations were recovered in low KCl (1 mM) aCSF for 1 hour
623 prior to dopamine application, (C). In a third experiment excitability was reduced by sequentially
624 increasing bath $MgSO_4$ concentration (1.0-2.5 mM) after evoking a rhythm with dopamine, (D). In a final
625 experiment, AP5 was bath-applied to antagonize NMDA receptors (5 µM) 20 minutes prior to addition of
626 dopamine. (E). An example cross wavelet frequency power spectrogram illustrates the degradation of
627 rhythmic activity when aCSF with dopamine and low KCl washed into the bath. (F). Regions of interest
628 were analyzed for cross wavelet spectrograms between left and right L2 and L5 neurograms around fast
629 and slow rhythm frequency bands. The power of the fast rhythm was reduced under all conditions in the

L2 (Fi) and L5 (Fii) neurograms. (Fiv). Slow rhythm power was reduced in the L2s but only reduced in the L5s by $MgSO_4$ and washing in low KCl. Data are presented as mean ± SD with asterisks denoting a significant difference between the respective point and the rhythm at 20 minutes following dopamine application. Non-parametric one-way ANOVAs were performed for fast or slow rhythms in L2 and L5 power. # denote significant differences on post hoc analyses between each respective condition compared to rhythm power from 50 µM of dopamine alone (#: $p < 0.05$, ##: $p < 0.01$, ###: $p < 0.001$).

Figure 6: Sequential enhancement of network excitation with NMDA modulates dopamine-evoked rhythmicity. (A). Neurograms recorded from left and right L2 and right L5 ventral roots illustrate the experimental paradigm and resultant effect on rhythmicity. Bath application of 50 µM of dopamine (DA) evoked a multi-rhythmic pattern of motor activity that is modulated as network excitation is boosted by sequentially increasing the concentration of NMDA in the bath (red arrows). When NMDA is increased to 6 µM, the pattern switches from multi-rhythmic, to a single, continuous locomotor-like rhythm. (B). The frequency power distribution following dopamine application and subsequent excitability manipulation is illustrated in the cross-wavelet frequency power spectrogram over time with frequency on the left Y-axis, time on the X-axis and increasing power represented as warmer colours. (C). At 6 µM NMDA, the pattern switches from multiple rhythms, to a single continuous rhythm. (D). Regions of interest were selected around the fast and slow rhythms and respective frequency and power for left and right L2 and L5 neurograms analyzed over time. Increasing network excitation increased the power of the fast rhythm and decreased the power of the slow rhythm. (E). The phase and regularity of the fast rhythm is presented in the circular plots in Ei and Eii and illustrate the switch to a locomotor-like pattern at 6 µM NMDA as the vector length increases and phase moves closer to 180 degrees in both the left and right L2s and ipsilateral L2-L5. The phase in circular plots is reported in degrees with 180 degrees indicating an alternating pattern and 0 degrees being synchronous. The length of arrows represent

654 mean vector length (r) or robustness of the pattern. Each dot represents the average phase for an
655 individual preparation for each respective experimental condition. Data are presented as mean ± SD
656 with asterisks denoting a significant difference between the respective point and the rhythm at 20
657 minutes following dopamine application (#: $p < 0.05$, ##: $p < 0.01$, ###: $p < 0.001$) using pairwise multiple
658 comparisons Tukey post hoc analysis when significant main effects on a repeated measures ANOVA
659 were found.

660

661 **Figure 7: 5-HT evokes multirhythmic patterns of motor activity that becomes locomotor-like as**
662 **network excitation is enhanced with KCl.** (A). Neurograms recorded in separate experiments from
663 single L2 ventral roots illustrate bath application of 10 µM 5-HT evokes a single slow rhythm (Ai), 15 µM
664 evoking a slow and fast rhythm (Aii) and 20 µM evoking a single fast rhythm (Aiii). (B). Autowavelet
665 spectrograms depicted in Bi-iii illustrate these rhythms. (C). Boosting network excitation following the
666 generation of multiple rhythms with 15 µM 5-HT caused a transition from a multi-rhythm to a single
667 locomotor-like rhythm. Network manipulations are represented and highlighted as red downward arrow
668 in the spectrogram. (D). Regions of interest were selected within cross-wavelet spectrograms around the
669 fast and slow rhythms and respective frequency and power for left and right L2 and L5 analyzed over
670 time. Boosting network excitation increased the power of the fast rhythm (Di) and decreased the power
671 of the slow rhythm (Div). (E). The bursting pattern of the fast rhythm is presented in the circular plots in
672 Ei and Eii and illustrates an increase in the vector length at 10 mM KCl in the left and right L2s and
673 ipsilateral L2-L5 at 8 mM KCl but at 10 mM the length declined as activity became tonic. The phase in
674 circular plots are reported in degrees with 180 degrees indicating an alternating pattern and 0 degrees
675 synchronous. The length of arrows representing mean vector length (r) and angle or robustness of the
676 pattern. Each dot represents the average phase for an individual preparation for each respective
677 experimental condition. Data are presented as mean ± SD with asterisks denoting a significant difference

678 between the respective point and the rhythm at 20 minutes following dopamine application (*: $p < 0.05$)
679 from Tukey post hoc analysis when significant main effects on a repeated measures ANOVA were found.

680

681 **Figure 8: Neuromodulators evoke rhythmicity by moving the network through an excitation**
682 **parameter space with the end point pattern being locomotor-like**. State 1 (basal state) in isolated
683 rodent spinal cords is characterized by spontaneous network activity. Depolarization of the network
684 moves the network into a higher excitation state (state 2) characterized by tonic activity with no
685 rhythmicity. State 3 is characterized by multi-rhythmic patterns of motor activity where modulator-
686 specific patterns of rhythmic motor activity may exist. Finally, in state 4, the locomotor state is
687 characterized by continuous rhythmic activity with an alternating locomotor-like pattern expressed as a
688 network emergent property at the highest level of network excitation. Neurograms depicted in the
689 schematic are from ventral root recordings in the right L5 and left and right L2 spinal segments. Curved
690 lines in the schematic represent transition zones between network states, where dopamine would be
691 expected to have the greatest effects on network output.

692

693 **Figure 9: Dopaminergic modulation of State 4**. Dopamine exerts a robust modulation of locomotor-like
694 activity at a position in the state space near a transition zone, however, overall the rhythm qualitatively
695 stays the same and the effect does not change when network excitation is manipulated. (Ai). An
696 unstable locomotor rhythm can be evoked by bath application of 10 µM 5HT and 5 µM NMA. (Aii).
697 Dopamine reduces the frequency and stabilizes the locomotor rhythm. (B). This is particularly evident in
698 the spectrogram. (C, D), Network excitation was manipulated initially as a means of evoking rhythms of
699 different frequencies but can also be interpreted as a network excitation state manipulation. (D).
700 Regardless of the baseline frequency, the modulatory effect of dopamine on rhythm robustness (power)
701 was the same. (E). The respective position of the network within the locomotor state under each

modulatory and excitability condition are plotted within the state space. These data have been previously published (Sharples et al., 2015) and we provide an updated interpretation of our findings in light of our current work.

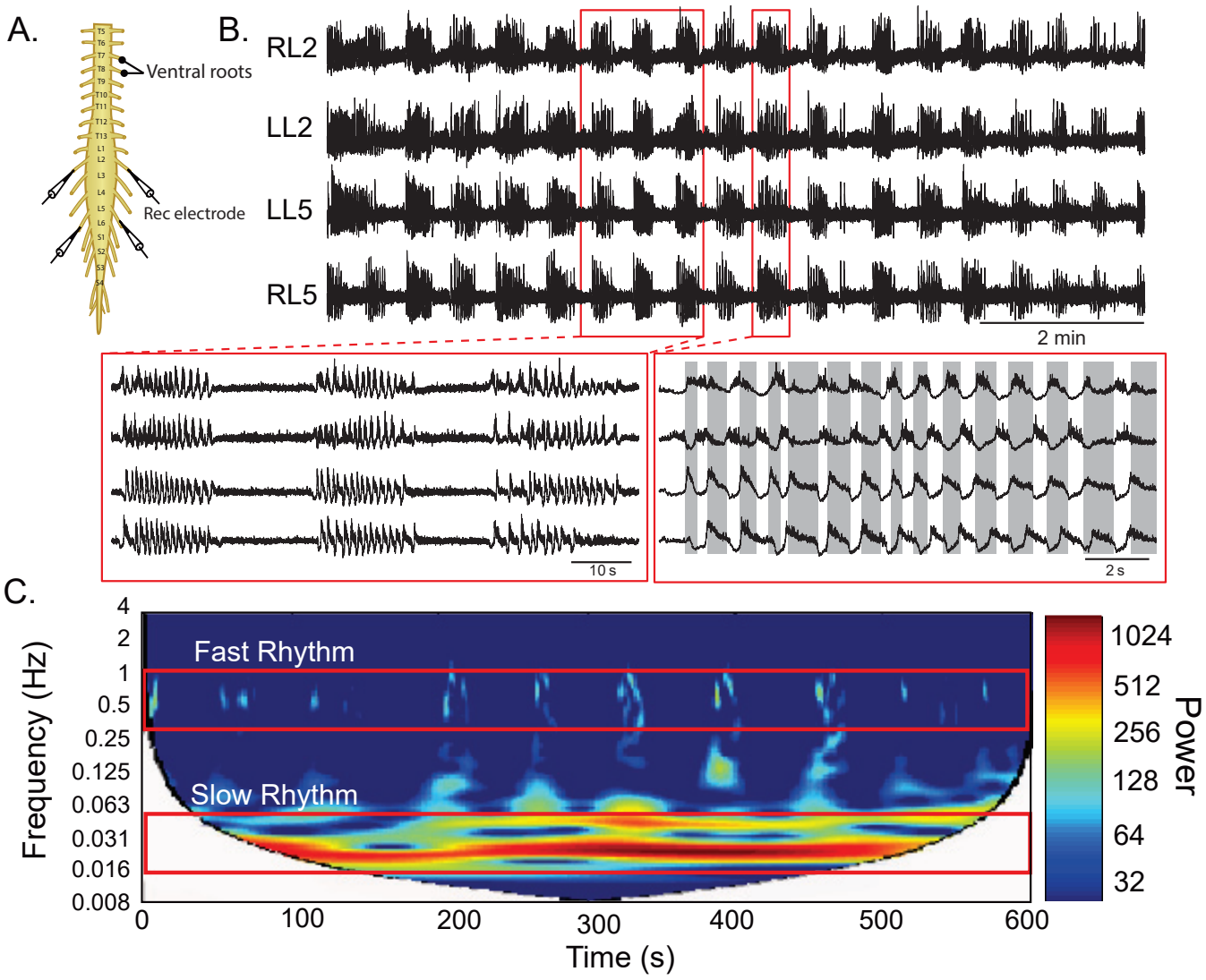

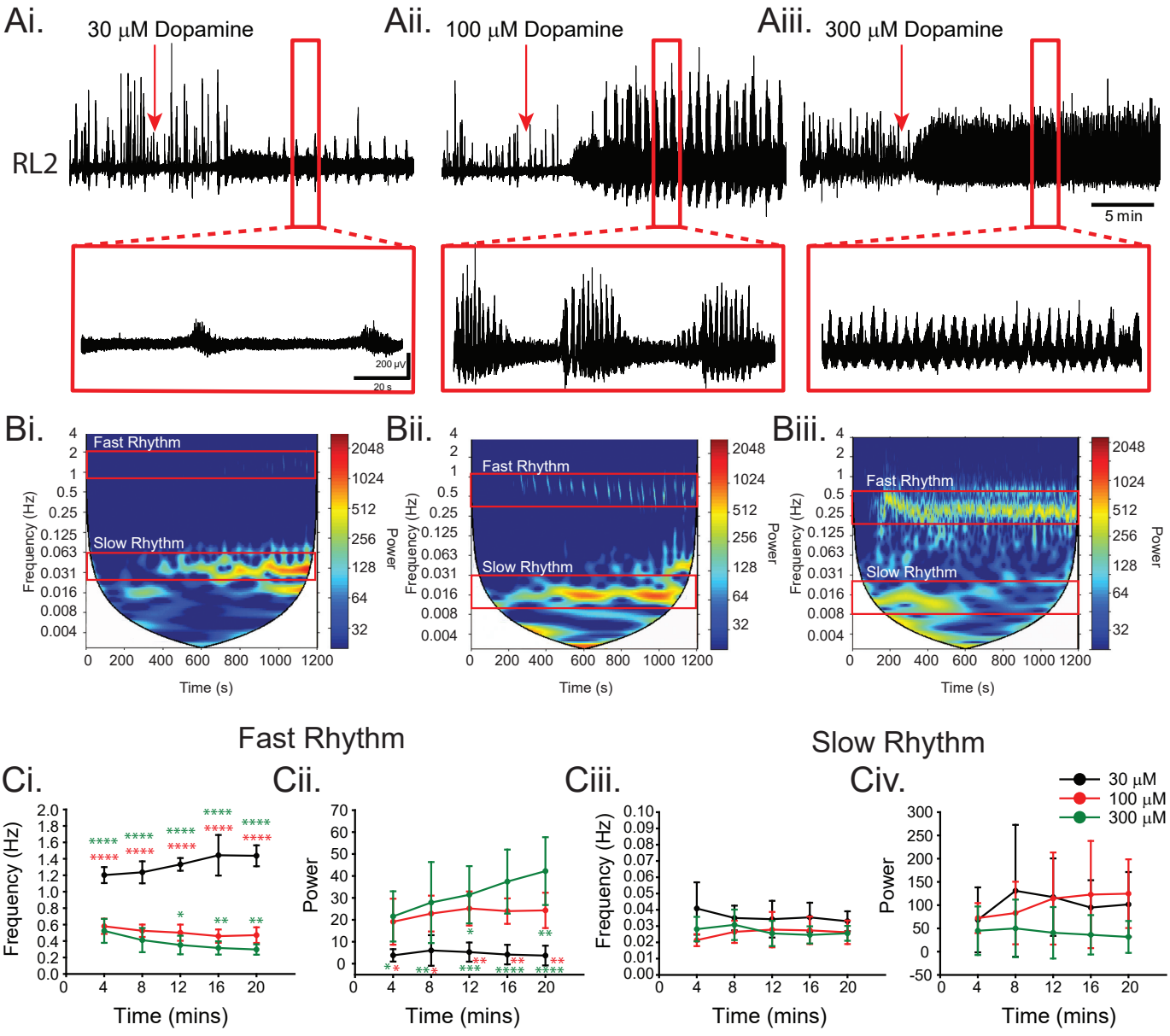

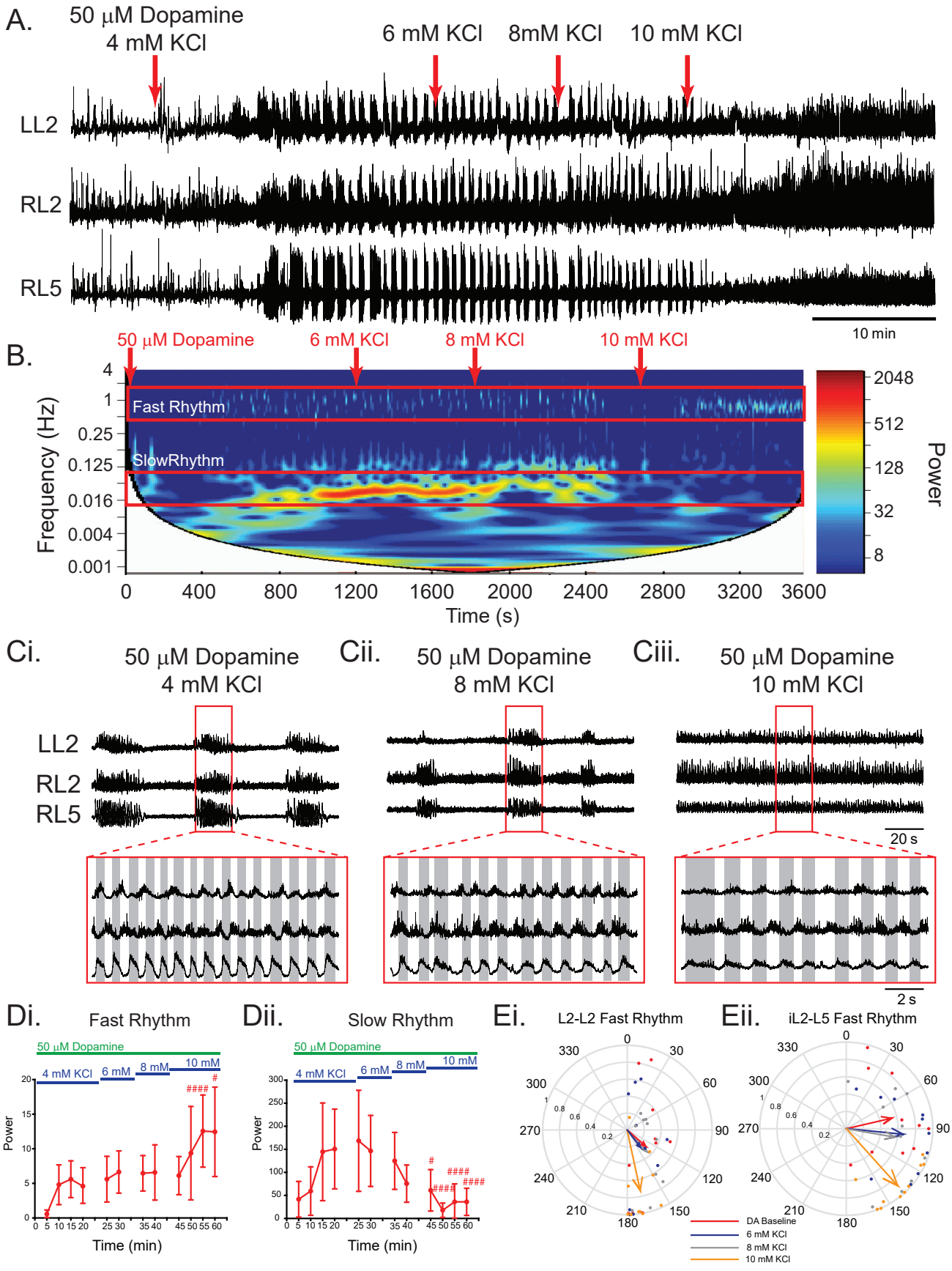

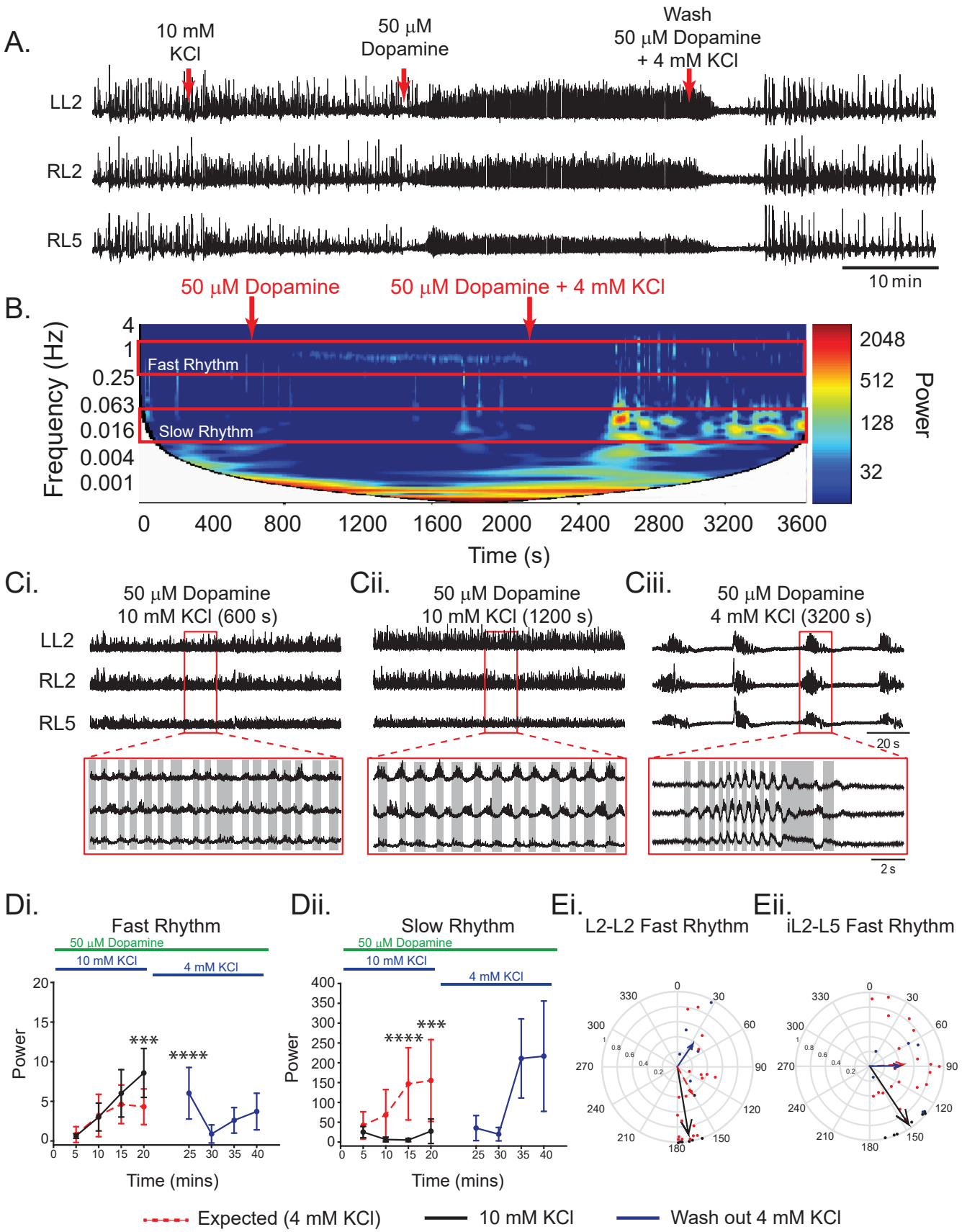

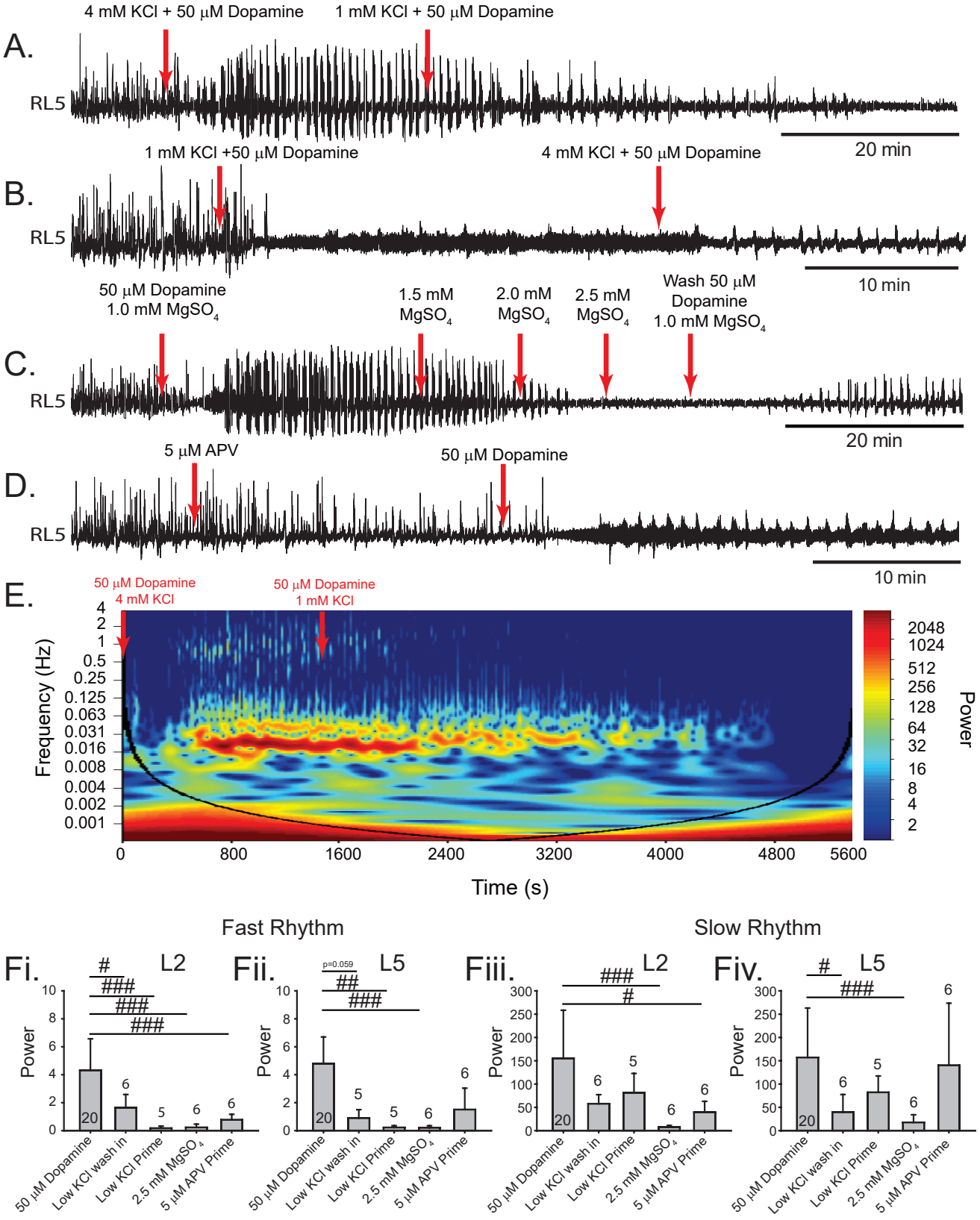

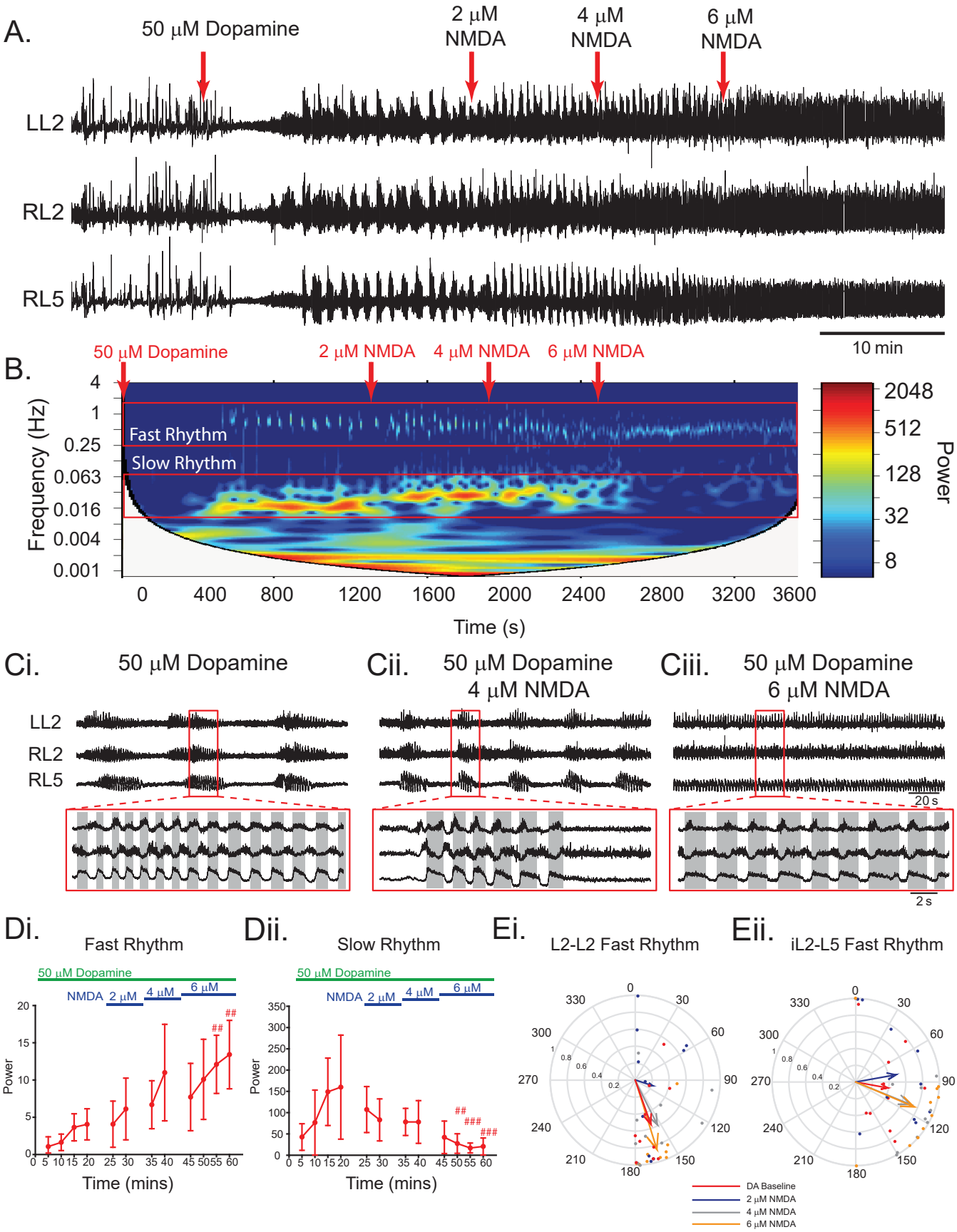

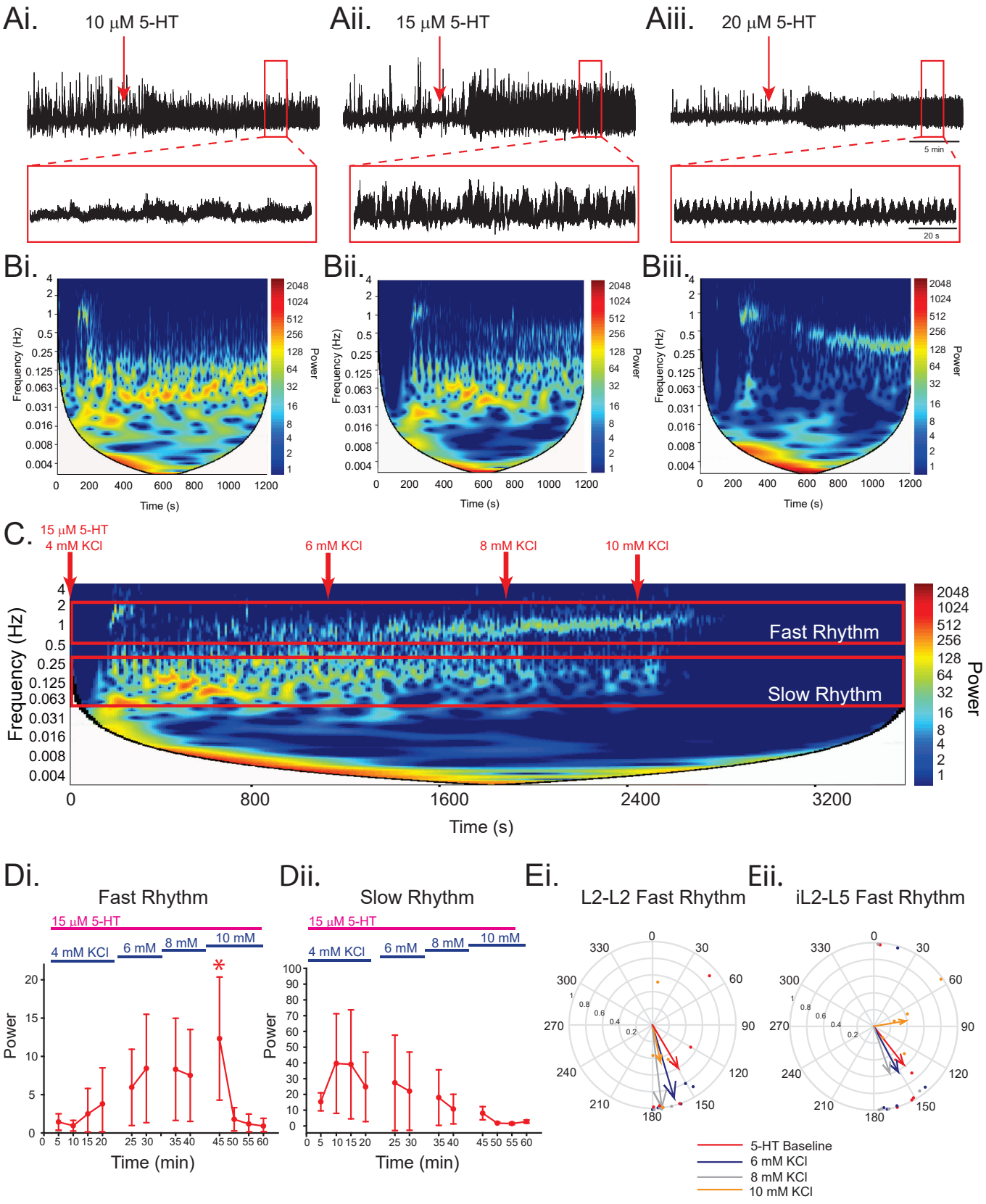

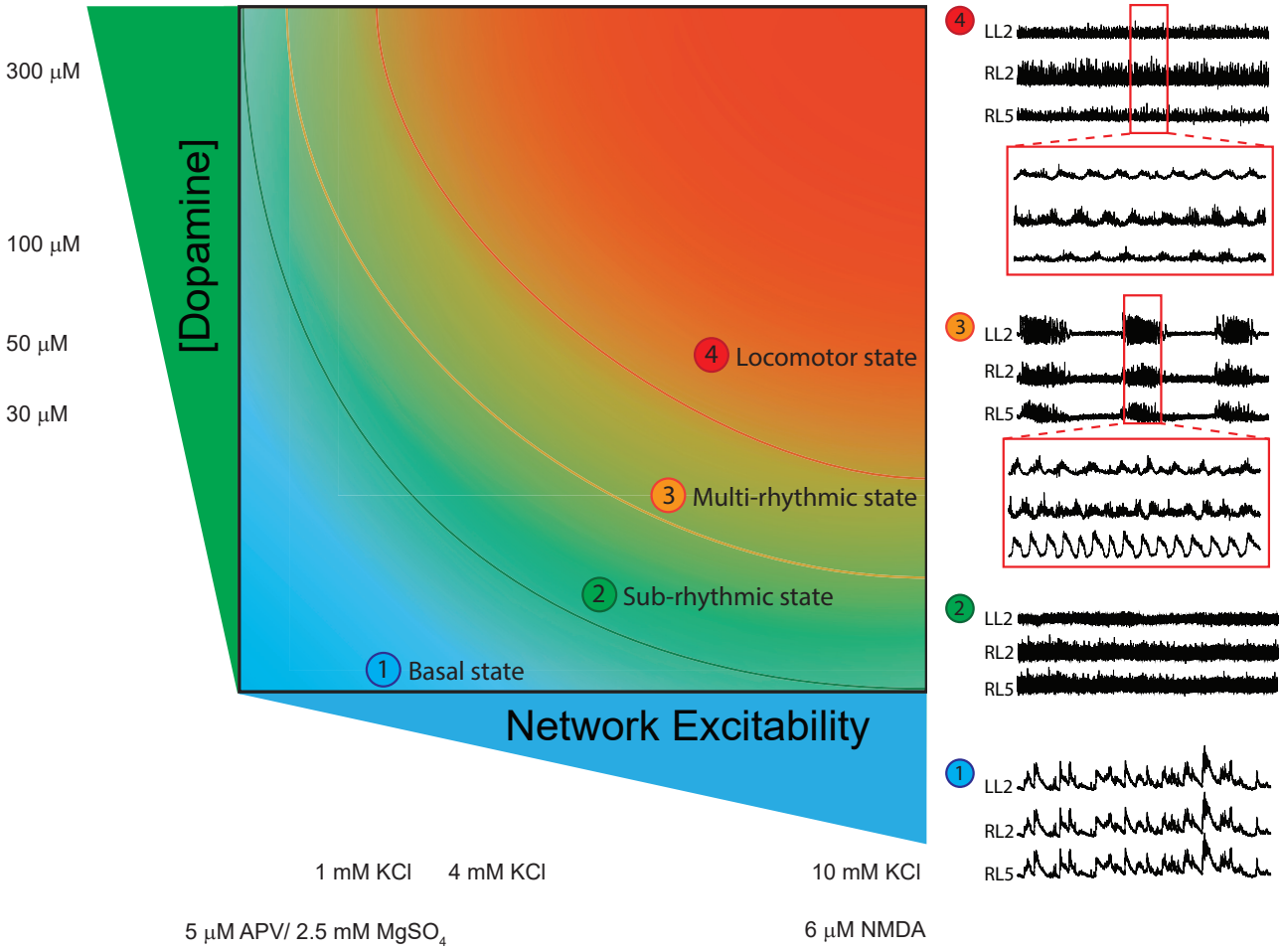

1. Basal state -Spontaneous activity characterized by stochastic episodes of tonic and rhythmic bursting
2. Sub-rhythmic state - tonic, no rhythmic activity
3. Multi-rhythmic state - multiple rhythms, diverse pattern
4. Locomotor state - single rhythm, locomotor pattern